Spindle Microtubules and Their Mechanical Associations after Micromanipulation in Anaphase

R. BRUCE NICKLAS, DONNA F. KUBAI, and THOMAS S. HAYS
Department of Zoology, Duke University, Durham, North Carolina 27706. T. S. Hays's present address is the Department of Zoology, University of North Carolina, Chapel Hill, North Carolina 27514.

ABSTRACT Micromanipulation of living grasshopper spermatocytes in anaphase has been combined with electron microscopy to reveal otherwise obscure features of spindle organization. A chromosome is pushed laterally outside the spindle and stretched, and the cell is fixed with a novel, agar-treated glutaraldehyde solution. Two- and three-dimensional reconstructions from serial sections of seven cells show that kinetochore microtubules of the manipulated chromosome are shifted outside the confusing thicket of spindle microtubules and mechanical associations among microtubules are revealed by bent or shifted microtubules. These are the chief results: (*a*) The disposition of microtubules invariably is consistent with a skeletal role for spindle microtubules. (*b*) The kinetochore microtubule bundle is composed of short and long microtubules, with weak but recognizable mechanical associations among them. Some kinetochore microtubules are more tightly linked to one other microtubule within the bundle. (*c*) Microtubules of the kinetochore microtubule bundle are firmly connected to other spindle microtubules only near the pole, although some nonkinetochore microtubules of uncertain significance enter the bundle nearer to the kinetochore. (*d*) The kinetochore microtubules of adjacent chromosomes are mechanically linked, which provides an explanation for interdependent chromosome movement in "hinge anaphases." In the region of the spindle open to analysis after chromosome micromanipulation, microtubules may be linked mechanically by embedment in a gel, rather than by dynein or other specific, cross-bridging molecules.

The exact, three-dimensional reconstruction of spindle microtubules is a daunting but rewarding venture. The most revealing information comes from tracing in serial thin sections tens or hundreds of individual microtubules in their entirety, to determine their length, position in the spindle, and proximity to other microtubules. An impressive example of the insights into spindle function that a detailed reconstruction can yield is the "near-neighbor" analysis of microtubules in the central spindle of a diatom (16, 19). The first steps toward a comparable reconstruction of microtubules in the kinetochore microtubule bundle have been taken (e.g., 9, 31, 38), but much remains to be done.

In principle, reconstruction of the whole spindle is not necessary for some purposes. Instead, attention might be concentrated on a single motile unit—one chromosome and the microtubules associated with it, reducing to a more manageable level the number of chromosomes, microtubules, and serial sections involved. The problem, of course, is how to distinguish unambiguously the microtubules associated with one chromosome from all other microtubules in the spindle. To help solve this problem, we used micromanipulation of a chromosome in a living cell to shift the position of the chromosome and to stretch it before fixation for electron microscopy. The shift in position moves both the chromosome and its kinetochore microtubules outside the confusing thicket of other spindle microtubules, and therefore aids in identifying them. The stress produced by stretching the chromosome is transmitted to its kinetochore microtubules and to all the other microtubules mechanically connected to them. This produces changes in position and bends in these mechanically connected microtubules, which make this group of microtubules identifiable. We report here some success in tracing individual microtubules and progress toward a three-dimensional reconstruction of microtubules in the kinetochore microtubule bundle.

Stretching a chromosome before fixation also allowed us to study the mechanical connections among spindle microtubules. The functional significance of microtubules is closely tied to their mechanical connections with one another and with other spindle components—the existence of connections is essential for a significant role in mitosis, and the character of the

THE JOURNAL OF CELL BIOLOGY · VOLUME 95 OCTOBER 1982 91-104

connections helps define the role or roles. The reconstruction of unaltered spindles can give clues to mechanical linkages among microtubules from their proximity to one another or from material between them, but only clues. A more direct approach is to observe the alterations in spindle organization caused by controlled mechanical stress. The structural consequences of experimentally applied stress have long been studied by light microscopy, from early centrifugation experiments designed to test the reality of the spindle as a mechanical unit (for review, see reference 36) to recent micromanipulation experiments probing the attachment of chromosomes to the spindle (1, 2, 29). Our electron microscopic observations on spindles subjected to stress by stretching a chromosome naturally permit the effects on microtubules to be seen rather than surmised. Mechanical connections among spindle microtubules are made visible by bent and displaced microtubules some distance from the stretched chromosome, providing evidence on the existence, frequency, site, and nature of the connections. The mechanical associations observed suggest an explanation for one type of interdependent chromosome movement and bear tangentially on current speculations in which a gel-like spindle matrix would generate the force which moves chromosomes. Some of these observations have been summarized in reports for meetings (26, 28).

In this paper "KMt" will sometimes be used for kinetochrome microtubule, and "non-KMt" for nonkinetochore microtubule—any other sort of spindle microtubule.

MATERIALS AND METHODS

Material

Spermatocytes from a laboratory colony of the grasshopper *Melanoplus differentialis* (Thomas) were cultured as previously described (25).

Light Microscopy, Micromanipulation, Ciné Recording, and Analysis

All these procedures were carried out as described previously (29), except that Agfa "Copex Pan Rapid" 16-mm ciné film was used. One special feature of the micromanipulation experiments should be noted. The micromanipulation needle was inserted into a chromosome and never touched spindle microtubules. A chromosome at the periphery of the spindle was chosen as the target, the needle was introduced directly above it, and the chromosome was then manipulated as described in Results. Thus, the microtubule rearrangements observed are due exclusively to the stress transmitted to microtubules by stress on the chromosome, not to direct contact with the needle.

Agar-treated Glutaraldehyde

BACKGROUND AND GENERAL REMARKS: As cultured for micromanipulation, the cells are covered by a layer of inert oil. A cell is fixed for electron microscopy at the desired moment during manipulation by injecting glutaraldehyde into the aqueous medium near the target cell. The overlying oil is then flushed away with large quantities of fixative, permitting further processing for electron microscopy by standard techniques (25). The spindles of smaller insect cells such as mole cricket spermatocytes are well-preserved after this procedure (11), so the technique itself causes no preservation problems. However, we were not satisfied with spindle preservation in the large cells of *Melanoplus* and other grasshoppers, especially after comparing *Melanoplus* spermatocytes fixed by injection of glutaraldehyde under the oil with cells fixed on a glutaraldehyde-agar substrate as described by LaFountain (12). Similar results had been obtained by others for crane-fly spermatocytes: cells fixed on the agar-glutaraldehyde layer contain about twice as many spindle microtubules (13) as cells treated more conventionally (6). The reason for this difference was not clear—LaFountain (12) used an agar substrate simply because more cells stick to agar than to uncoated glass, and added glutaraldehyde to the agar so that fixation would begin as soon as the cells contacted the substrate.

We investigated the unlikely possibility that the agar in LaFountain's procedure somehow improves glutaraldehyde as a fixative for microtubules and were surprised to find that it does. When "agar-treated glutaraldehyde" (prepared as described below) is used in our injection procedure, numerous non-KMts are seen in every thin section of the spindle of *Melanoplus* spermatocytes, while in cells fixed by the identical procedure with untreated glutaraldehyde, non-KMts are very rarely seen. The number of KMts is also increased: from 18 to 22 per kinetochore using untreated glutaraldehyde to an average of 45 (Table I, below) in cells fixed with agar-treated glutaraldehyde. Also, the spindle matrix is richer in structural detail when agar-treated glutaraldehyde is used. (Sample micrographs are shown in Figs. 1*c* and 4*c*.) Agar-treated glutaraldehyde is not a universally useful elixir, however. Preliminary observations suggest that the spindle in the relatively small spermatocyte of a cricket (*Acheta domestica*) is equally well-preserved in treated or untreated glutaraldehyde. In collaboration with Dr. Kent McDonald, microtubule preservation has been quantitatively investigated in the cultured cells of a marsupial mammal (*Potorous tridactylis*, cell line PtK_2). Counts of microtubules in cross-sectioned spindles of early anaphase PtK_2 cells were nearly equal in cells fixed in treated or untreated glutaraldehyde. These results with smaller cells are not surprising if it is assumed that their spindles are already well-preserved with untreated glutaraldehyde—perhaps we were trying to improve on perfection.

We remain ignorant of the reasons for improved microtubule preservation in grasshopper spermatocytes. Osmolarity, ultraviolet and nuclear magnetic resonance spectra, and the calcium concentration of glutaraldehyde solutions are not detectably affected by agar treatment. Nevertheless, we have a good reason, independent of improved preservation, to believe that agar treatment produces a real alteration in the properties of the fixative. Fixation of cells under oil necessitates repeated contact of the injection pipette with the medium around the cells. The medium is rich in cellular debris, which reacts with the glutaraldehyde at the tip of the pipette, forming aggregates that stick to the tip and eventually clog the pipette. If the pipette contains agar-treated glutaraldehyde, clogging is far more likely than with untreated glutaraldehyde. This is not a subjective impression: the difference is so great, and clogging such a bother, that to try both fixatives will quickly convince anyone that the difference is real. We suspect that pipettes loaded with agar-treated glutaraldehyde are so easily clogged because the treatment increases the reactivity of glutaraldehyde with cellular debris, which may be related to the improved fixation of larger cells.

PREPARATION: The ingredients are freshly prepared 0.5% purified agar (Difco Laboratories, Detroit, MI; no. 0560-02) in distilled water, and 24% glutaraldehyde, prepared by diluting with distilled water, 70% glutaraldehyde from sealed glass ampules (Ladd Research Industries, Inc., Burlington, VT; no. 20150; we use only lots with an optical density ratio—$OD_{230\ nm}/OD_{280\ nm}$—of less than 0.2). The agar is prepared first, and set aside at 4°C to gel. 50 ml of 0.5% agar and 23.3 ml of 24% glutaraldehyde are combined, broken up into a slurry with a glass rod, and mixed on a rotary shaker at ~200 rpm for 30 min at 4°C. The glutaraldehyde is then separated from the agar by vacuum filtration through coarse filter paper in a Büchner funnel. The concentration of the recovered, "treated" glutaraldehyde is calculated from its optical density at 280 nm, using the optical density of the initial, 24% glutaraldehyde as a standard. A typical yield is 22 ml of glutaraldehyde at a concentration of 11%. The treated glutaraldehyde is stored at 4°C, and aliquots are appropriately diluted with a buffer/NaCl stock solution each day, to give buffered glutaraldehyde at the final concentration desired. Fresh agar-treated glutaraldehyde is prepared each week.

Electron Microscopy

Except for the substitution of agar-treated for untreated glutaraldehyde, the cells were fixed and prepared for electron microscopy as detailed in reference 25, using these variants described therein: the short-duration, PIPES buffer schedule was used for fixation, the oil over the cells was removed by injecting a relatively large volume of fixative under the oil and then flushing the surface with additional fixative, and the cover slip was removed after embedding by Moore's (23) hydrofluoric acid method. Unmicromanipulated control cells were fixed and prepared exactly as manipulated cells. Cells were serially sectioned in a plane longitudinal to the spindle axis at a thickness of 80–90 nm and mounted and stained by standard procedures (10).

The serial sections were examined in a Siemens 101 or a Zeiss 10A electron microscope operated at 80 kV, and micrographs were made on 70mm roll film (Kodalith LR 2572) at a magnification of 3,100 to 3,200 (determined for every cell from a micrograph of a grating replica). An aerial film viewer (Hoppmann Corp., Springfield, VA) was used in examining micrograph negatives and in preparing reconstructions. The viewer projects an image of the micrograph on a large (74 × 74 cm), high resolution screen at a magnification of 14 or 31 times the original electron microscope magnification.

Chromosomes and microtubules in the vicinity of the micromanipulated chromosome were reconstructed in seven cells by the following procedure. The image of the first micrograph from a series of serial sections is projected on the screen of the viewer. A transparent polyester plastic sheet is placed over the screen and microtubules and chromosome outlines are traced on the sheet. Three or four crossed lines are added to the sheet to serve as registration markers. While

the tracing of the first section remains on the screen, the image of the second section is projected and roughly aligned with the tracing using the chromosome outlines as landmarks. Then the alignment is adjusted using continuity of microtubules as the guide. The aim is to maximize the number of perfect matches between microtubule ends in contiguous sections: the tracing is moved about until the best fit is obtained between the ends of the microtubule profiles in the tracing with those in the projected image. Alignment is facilitated by giving special attention initially to a few microtubules which are distinctive, e.g., those that traverse the spindle at a different angle than most. Once this best fit is obtained, a second sheet of plastic is laid over the original tracing, and the registration markers, chromosome outlines, and microtubules of the second section are traced. This process is repeated for all sections in the set to be reconstructed. To improve the accuracy and completeness of the reconstruction, the tracing-image comparisons are then repeated in reverse. The original set of tracings is used, but now, beginning with the last section of the series, the tracing of an even-numbered section is compared with the projected image of the next lower odd-numbered section—the reverse of the original comparison. During this reverse analysis, an independent set of registration markers is added and so are any previously overlooked microtubule segments.

The presence of the tracing from one section while information from the next is being recorded is a valuable guide: very short segments of microtubules which are continuations of microtubules in the previous section are seldom overlooked—the lines on the original tracing serve as pointers which indicate precisely where to look for microtubule continuations. The registration procedure could be biased in favor of the continuation or termination of one or a few selected microtubules, but only if the obvious misalignment of numerous other microtubules that would result were ignored. Reproducibility is good: when the tracing-tracing alignment is compared using the two independent sets of registration markers (those assigned for the initial tracing and those added during the reverse analysis), the alignments are the same to within one microtubule diameter >90% of the time. Less satisfactory reproducibility results from occasional distortion in one section which makes impossible an exact match of microtubule ends over the whole of that section relative to the two on either side. The problem is dealt with by using multiple registration markers to match up small areas of the distorted section with their counterparts in the adjacent, undistorted sections. Registration accuracy has been estimated not only from alignment reproducibility, but also directly, from how well the ends of unambiguously recognizable microtubules match up in tracings of adjacent serial sections. (The "unambiguous" class includes microtubules at odd angles in areas with relatively few other microtubules, as well as certain curved microtubules resulting from micromanipulation; for examples of the latter, see Fig. 8 and associated text, below.)

For the two-dimensional reconstructions considered in this report, an alignment accuracy of ±2 microtubule diameters was considered acceptable, and ±1 microtubule diameter was usually achieved. This gives an indication of microtubule continuity or termination adequate for most of our purposes. When necessary for exact tracking of particular microtubules, greater care in alignment was taken to meet a more stringent standard—a registration accuracy of plus-or-minus half the diameter of a microtubule over a few sections. This level of accuracy was achieved for the microtubules shown in the three-dimensional reconstructions in this report. Even when the required accuracy in alignment is achieved, following every microtubule from one end to the other is extremely time consuming, because even small segments in every section must be found and traced in a large number of sections. Fortunately, this was not necessary to achieve most of our goals, but a few particularly interesting microtubules have been traced in their entirety in the three-dimensional reconstructions; these are identified in the Results section. The true length of all other microtubules is unknown.

Two-dimensional reconstructions were examined simply by stacking the tracings with the registration marks aligned; for publication (see Figs. 2 and 5), a composite tracing of the stacked set showing all the microtubules but only some chromosome outlines was prepared and photographed. Three-dimensional reconstructions of selected but representative (see Results) microtubules were prepared by the computer-assisted techniques described by Moens and Moens (22), using their programs and equipment. Using tracings of several sections, the x and y coordinates of microtubules, chromosome outlines, etc., on each tracing are entered into the computer from a digitizer, along with the number of the section from which the tracing was made. The computer generates smoothed lines connecting the coordinates and a view of the reconstruction at any chosen angle. Plots of a view in the original sectioning orientation and a view rotated 10° are presented as stereo pairs (see Figs. 3, 6, and 8; while the actual section thickness was 80–90 nm, a section thickness of 150 nm was assigned for the computer plots to enhance the perception of depth). Note that the micrographs show a flat projection of microtubules in sections which are about three times thicker than the diameter of the microtubule, and we do not know where a given microtubule lies within the thickness of a section. The computer calculates an estimated path through the thickness of each section, based on the continuation or termination of that microtubule in adjacent sections. The resulting uncertainty about exactly where each microtubule is in three-dimensional space would be unacceptable if close associations between microtubules were in question. As it happens, however, the closest microtubule-microtubule associations we found involve microtubules separated from one another by about the thickness of a section or more. Hence, while information on microtubule position within the section could be obtained from stereo micrographs of tilted sections, that would have added nothing to the present investigation.

The number of kinetochore microtubules at their insertion into the kinetochore was counted in tracings in register, so that the end of each KMt could be tracked into the kinetochore. Tracking difficulties in this region of high microtubule density limit the accuracy, but the numbers (see Table I) are reliable to within ±10% (estimated directly from the maximal number of uncertain tracking assignments). Counts of microtubules in the KMt bundle at various distances from the kinetochore (see Table III) were made as follows. A template was constructed on a clear plastic sheet by drawing a rectangle enclosing the KMt bundle, lines at 1, 4, and 8 μm from the kinetochore, and registration marks corresponding to those on the tracings for reconstructions described above. The template was brought into register with the tracing of the microtubules from one section, and the number of microtubule profiles crossing the lines at 1, 4, and 8 μm from the kinetochore was counted (in cell 5, a later stage in anaphase, the KMt bundle merged with the spindle beyond 4 μm, so counts were made only at 1 and 4 μm). The procedure was repeated for the tracing of the next section and so on. The size of the template and the number of sections examined were chosen to include a generous volume around the KMt bundle, so that KMts which diverge somewhat from the rest at 4 or 8 μm from the kinetochore would not be excluded. (Hence, some non-KMts are included in the counts, and the number at 1 μm from the kinetochore is greater than the number of KMts actually inserting into the kinetochore.) The measurements of length reported in Table IV were made on the two-dimensional reconstructions, using an electronic planimeter (Numonics Corp., Lansdale, PA; model 1224). No allowance was made for foreshortening due to projection in a plane (for a microtubule 10 μm long as measured, and extending through 10 sections each 85 nm thick, the correction for the third dimension would add only 0.04 μm to its length).

RESULTS

The experimental design is as follows: a chromosome is snagged with the micromanipulation needle, displaced laterally, stretched, and later the cell is fixed for electron microscopy. Then, serial sections are cut and spindle microtubules in the vicinity of the stretched chromosome are reconstructed. Observations from seven cells are discussed in this report.

Mechanical Associations among Spindle Microtubules

Observations on two cells will be described in detail, followed by a summary including information from all seven cells.

CELL 1. Prints from the ciné record (Fig. 1 *a*) show the cell in life just before micromanipulation began (0.0-min print), after displacement and stretching of one chromosome (6.5-min print), and after fixation (10.1-min print). The manipulation needle was moved far to the left after snagging the chromosome, stretching it greatly (compare the 0.0- and 6.5-min prints, Fig. 1 *a*). The stress from stretching the chromosome was in a direction that caused the kinetochore of the manipulated chromosome to continue to point directly toward the pole (Fig. 1 *a*). The fixative was applied while the chromosome was still under tension, preserving the stretched configuration with relatively little relaxation (Fig. 1 *a* and *b*).

The chromosomes seen in life (Fig. 1 *a*) can all be identified in the survey electron micrograph from one section of a complete serial set (Fig. 1 *b*). A higher magnification micrograph (Fig. 1 *c*) is included to give some idea of the quality of preservation. The kinetochoric end of the manipulated chromosome is shown, along with several microtubules extending poleward (Fig. 1 *c*). Some of these microtubules insert in the kinetochore, an area of lower electron opacity than the body of the chromosome.

A two-dimensional reconstruction of the spindle in the vicinity of the manipulated chromosome is shown in Fig. 2. Most KMts of the manipulated chromosome (on the left) run straight

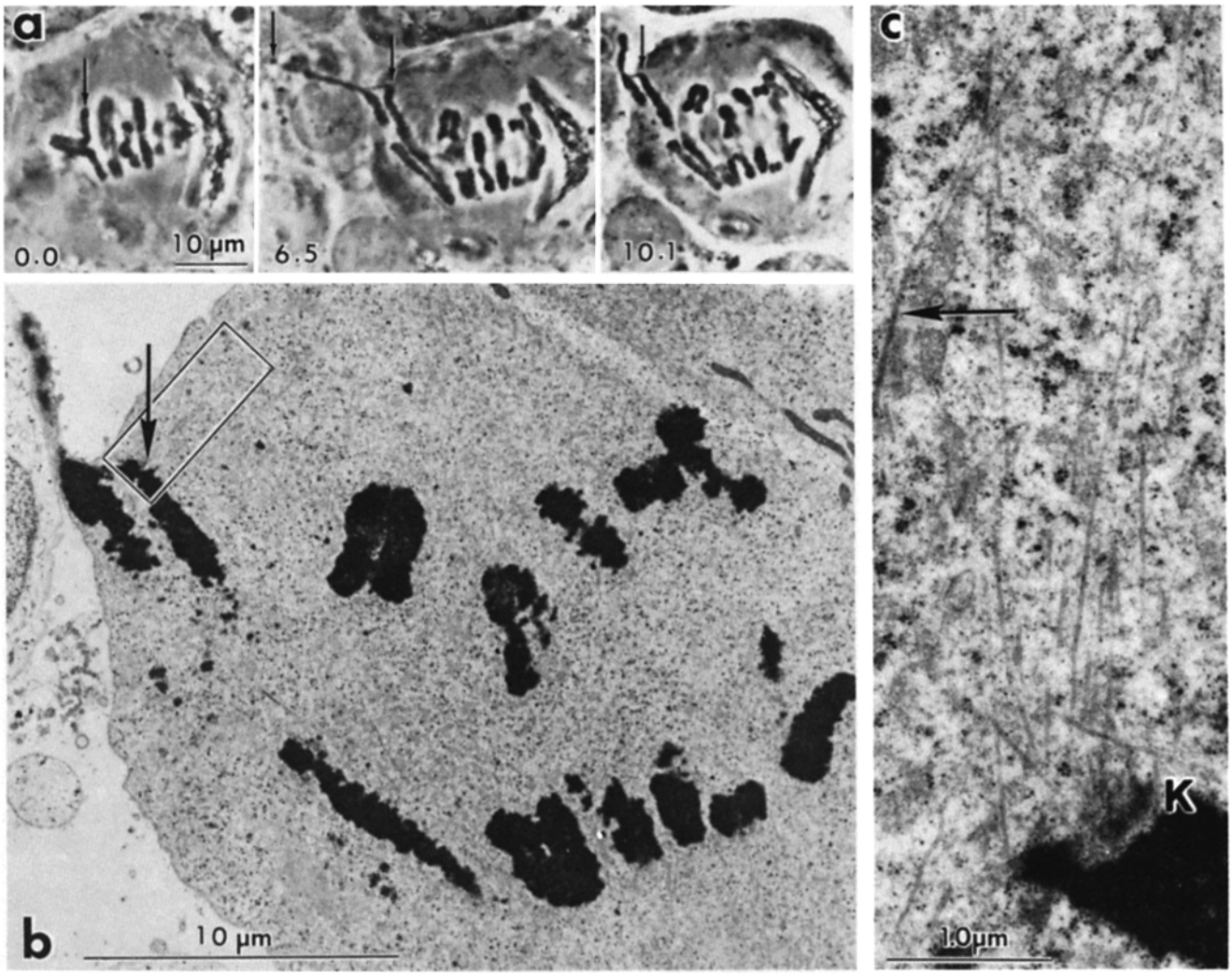

FIGURE 1 Light and electron microscopy of cell 1. (*a*) Prints from the ciné record of the cell in life and after fixation. The time in minutes is given on each print. An arrow in each print indicates the kinetochore end of the micromanipulated chromosome; in the 6.5-min print, a second arrow (at the left) indicates the stretched end of the chromosome. The cell is shown in the 0.0-min print at early anaphase, just before micromanipulation began. The 6.5-min print shows the cell during micromanipulation: a chromatid lying at the periphery of the spindle had been snagged with the needle and moved to the left, displacing and stretching one chromosome. The chromosome was held in the stretched configuration for 8.4 min. Tension was maintained as the cell was fixed (10.1-min print), and hence the stretched configuration as preserved with little alteration, although the stretched end was swept upward by the flow of fixative around the cell after the needle was removed (see also *b*). The volume of fixative added initially was greater than optimal, causing the cell to round-up somewhat. Electron microscope observations (not shown) disclose that despite the extension of the chromosome far beyond the cell body, plasma membrane completely encloses the stretched chromosome. × 1,000. (*b*) Survey electron micrograph at the level of the manipulated chromosome, and showing the chromosomes seen in life. The arrow indicates the kinetochore of the manipulated chromosome. × 4,500. (*c*) Higher magnification electron micrograph of the area enclosed in the box on *b*, but a different section of the complete serial set. The kinetochore (*K*) of the manipulated chromosome is shown, along with several microtubules extending poleward. The arrow indicates a portion of a curved microtubule traced in its entirety in the three-dimensional reconstruction (Fig. 3, microtubule 1). × 24,200.

toward the pole, identified by the position of pericentriolar material. The KMts of the immediately adjacent chromosome, however, follow a strikingly different path: they curve toward the KMts of the manipulated chromosome before continuing on toward the pole. Thus, the stress applied toward the left on the manipulated chromosome shifted in that direction not only its KMts, but also the poleward third of the adjacent chromosome's KMts. Hence these two groups of KMts must have been mechanically connected with one another near the pole. This effect extended no further across the spindle, however: the KMts of the chromosome on the right run straight toward the pole.

Nonkinetochore microtubules are seen most clearly in Fig. 2 between the manipulated chromosome and the one adjacent to it. Several non-KMts appear to enter the KMt bundle of the manipulated chromosome. In fact, only four of these actually enter the KMt bundle within 7 μm of the kinetochore. The other non-KMts seen in this region (Fig. 2) are in sections above or below the kinetochore microtubules. The only region in which kinetochore microtubules come close to numerous other spindle microtubules is near the pole—in the last 3 to 4 μm of a total kinetochore-to-pole distance of 11 μm. It is noteworthy that the non-KMts in the vicinity of the curved kinetochore microtubules of the adjacent chromosome were unaffected by the stress on the manipulated chromosome—these non-KMts are straight, not curved.

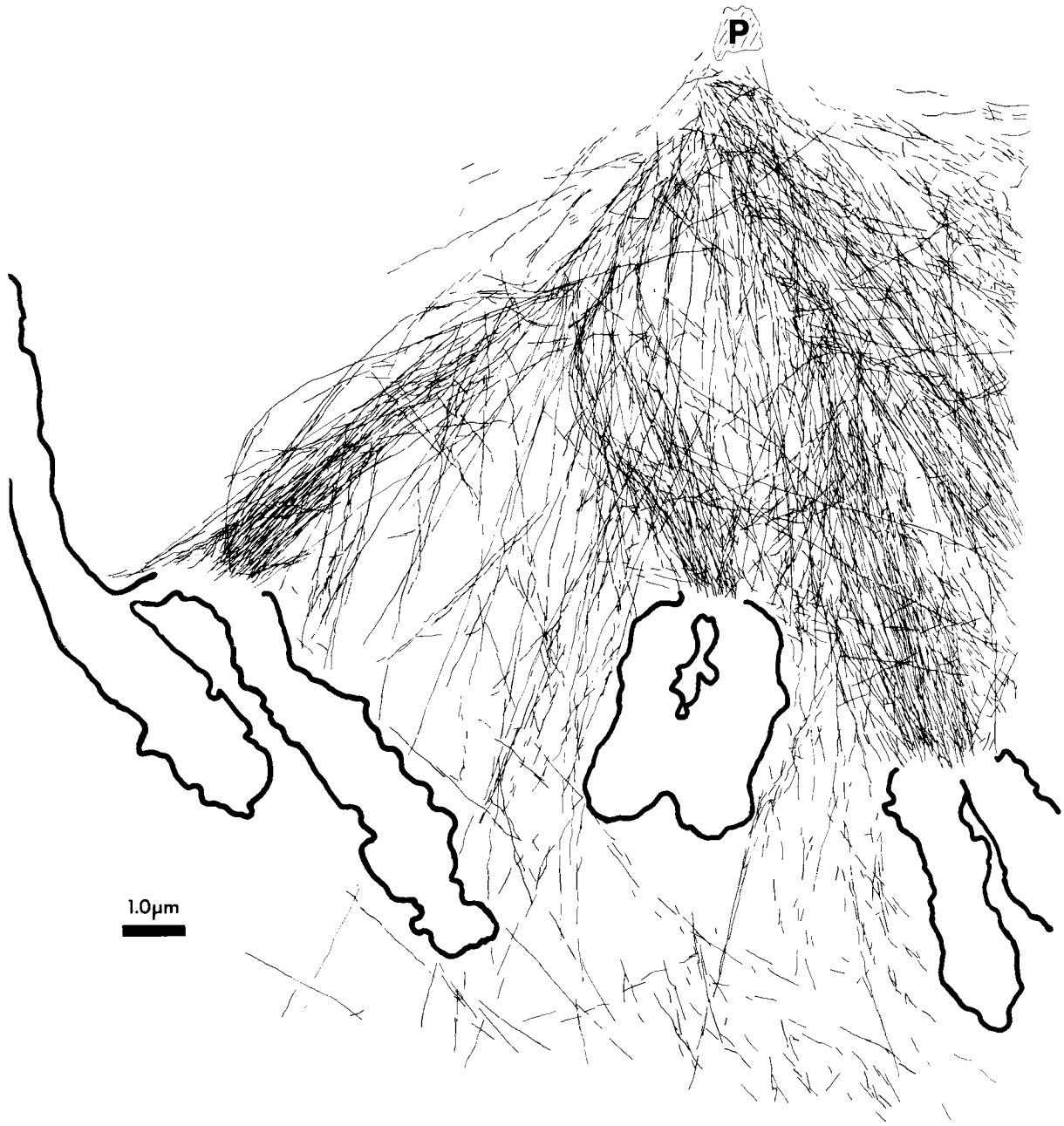

FIGURE 2 Two-dimensional reconstruction of part of the spindle of cell 1. The micromanipulated chromosome (left) and two adjacent chromosomes are shown in outline as broad lines, microtubules as thin lines, and pericentriolar material at the pole is labeled *P*. The orientation of the spindle is the same as in Fig. 1 *b*. Most kinetochore microtubules run straight toward the pole, while those of the immediately adjacent chromosome are strikingly curved—bent toward the KMts of the manipulated chromosome. The KMts of the chromosome on the right, farther from the manipulated chromosome, run straight toward the pole. A few nonkinetochore microtubules are seen, especially between the manipulated chromosome and the one closest to it. Information included in this reconstruction was derived from micrographs of 21 serial sections, starting with the section from which the pericentriolar material was traced; the microtubule tracings shown were from 18 serial sections, numbers 4 to 21 of this series (these sections were chosen to include the KMts of the manipulated chromosome plus sections on either side—KMts of the manipulated chromosome insert into the kinetochore in sections 8 to 15 of this series). All the microtubules noticed in the micrographs have been traced, but the full length of each is not necessarily shown (see Material and Methods). The microtubules appear to terminate short of the pericentriolar material, but this is misleading—this area of the spindle was not included in most of the micrographs analyzed.

A few microtubules oblique to the main spindle axis are evident in Fig. 2, especially on the right side. The oblique microtubules are not a consequence of the micromanipulation, since they occur in unmanipulated control cells in about the same number.

Fig. 3 shows a three-dimensional reconstruction of some microtubules associated with the micromanipulated chromosome and the adjacent chromosome. Note especially the path of the KMts of the adjacent chromosome as they curve upward and to the left toward the KMts of the manipulated chromosome. As a rule, the adjacent chromosome's KMts which are closest to those of the manipulated chromosome are bent the

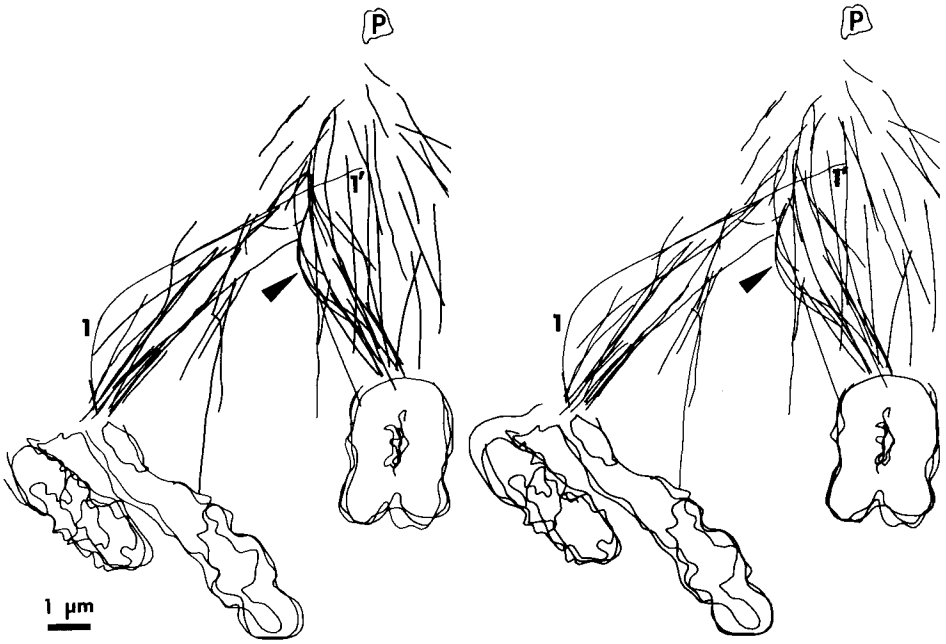

FIGURE 3 Three-dimensional reconstruction (stereo pair) of cell 1, showing some of the microtubules associated with the micromanipulated and the adjacent chromosome. The orientation is the same as in Figs. 1 *b* and 2, and the same set of serial sections was used as for Fig. 2. Most of the kinetochore microtubules of the manipulated chromosome (left) run straight toward the pole, while those of the adjacent chromosome curve upward and to the left (arrowhead) before curving back toward the pole (*P*: pericentriolar material). The microtubules labeled *1* and *1'* have been tracked through their full length (cf. Fig. 8).

most. Despite an exhaustive search, we have found no evidence for firm, short linkages between individual microtubules which could account for the observed bending of these kinetochore microtubules toward those of the manipulated chromosome. For example, consider the most sharply curved microtubules identified by the arrowhead in Fig. 3. If other microtubules were closely linked to these curved ones, they should lie nearby and should be similarly curved. No such microtubules are seen. (For clarity, only a few microtubules could be included in Fig. 3, but a representative sample is shown, including every microtubule in the vicinity of those identified by the arrowhead—cf. Fig. 2, in which all microtubules are shown.)

CELL 2: The micromanipulation experiment in cell 2 (Fig. 4*a*) differed in two ways from that in cell 1. First, the manipulated chromosome was stretched only briefly, but greatly, as shown in the 3.5-min print, Fig. 4*a*. Secondly, the tension on the chromosome was not along the original kinetochore-to-pole axis. The micromanipulation needle was moved diagonally relative to the spindle axis, stretching the chromosome toward the upper pole as well as away from the spindle. This forced the kinetochoric end of the manipulated chromosome to point toward the middle of the spindle (Fig. 4*a*, 2.0- and 3.5-min prints), not directly toward the pole. Some of the chromosomes seen in life are visible in the survey electron micrograph, Fig. 4*b*. A higher magnification micrograph, Fig. 4*c*, shows the kinetochore of the manipulated chromosome and some kinetochore microtubules. The kinetochore protrudes from the end of the chromosome—a common effect of stretching a chromosome greatly. A microtubule at the left in Fig. 4*c* extends toward the center of the spindle before curving to the right, toward the pole. As shown in the two-dimensional reconstruction, Fig. 5, many microtubules follow this trajectory, giving the bundle as a whole the appearance of a hammock hung between the kinetochore and the pole. Thus, the distance from the kinetochore to the centriole along the path of the leftmost kinetochore microtubules in Fig. 5 is greater than the length of a straight line between kinetochore and pole: 12.4 vs. 11.7 μm.

As already noted, kinetochore microtubules intermingle near the pole with those of the rest of the spindle. The most distinctive feature of cell 2 is the presence nearer the kinetochore of numerous nonkinetochore microtubules associated with the kinetochore microtubule bundle. The arrows in Fig. 5 identify five single microtubules or groups of three to five microtubules which appear to enter the KMt bundle. In fact, they do enter the bundle, rather than pass above or below it, as is clearly shown in the three-dimensional reconstruction, Fig. 6. (Here again, for clarity, only a small sample of the microtubules can be shown in stereo, but representatives of all microtubule types have been included—cf. Fig. 5.) Individual non-KMts can be traced in Fig. 6 from left to right, as they enter the bundle, pass among the KMts and terminate within the bundle or a short distance beyond. Most non-KMts run at an oblique angle to the KMts, but a few curve and become nearly parallel to the KMts (e.g., the microtubule identified by an arrowhead, Fig. 6). We have not observed even one example of close apposition between one of these nonkinetochore microtubules and a kinetochore microtubule. Even the few non-KMts which bend to become parallel with the KMts are not associated with a particular KMt which has the same curvature nor do non-KMts lie within a microtubule diameter or two of a KMt over any significant distance (Fig. 6; the sample of microtubules in Fig. 6 includes all kinetochore microtubules found near the nonkinetochore microtubules shown in the figure).

A suggestion of periodicity in the association of nonkinetochore microtubules with the kinetochore microtubule bundle is noticable in Fig. 5. Starting at the kinetochore and progressing poleward (upward in Fig. 5), non-KMts enter the bundle at intervals of ~1 μm. No such periodicity has been seen in any other cell, however.

The spindle properties observed in cells 1 and 2 have been confirmed in others, as follows:

(*a*) Kinetochore microtubules of the manipulated chromosome encounter large numbers of other microtubules only near the pole—in the 2–4 μm length of the kinetochore microtubule bundle nearest the pole (measured in 4 cells, including cell 1).

(*b*) A few nonkinetochore microtubules enter the bundle of kinetochore microtubules closer to the kinetochore. Cell 2 provides by far the most striking examples of this class of

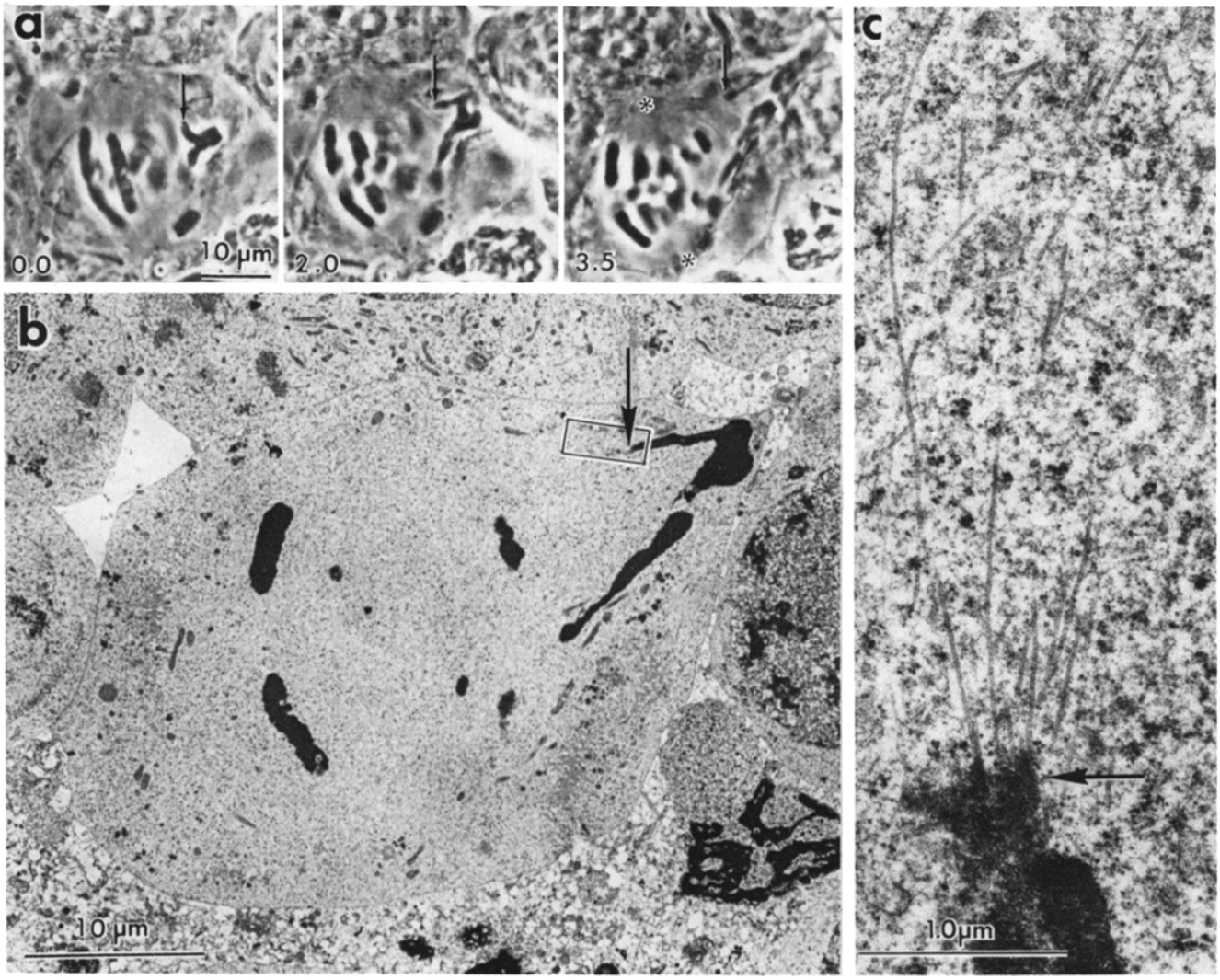

FIGURE 4 Light and electron microscopy of cell 2. (*a*) Prints from the ciné record showing the cell in life. The time in minutes is given on each print and the arrow indicates the kinetochoric end of the micromanipulated chromosome. The cell is seen at the start of anaphase before manipulation began (0.0 min), just after the chromosome on the right was stretched (2.0 min), and after relatively great tension was established (3.5 min; fixation began 4 s later). The approximate position of the poles is shown by asterisks on the 3.5-min print so that the angle at which tension was exerted may be compared with the spindle axis. The chromosome was subjected to moderate tension for 0.7 min and to greater tension for 0.7 min more. × 1,000. (*b*) Survey electron micrograph at the level of the manipulated chromosome (kinetochoric end at arrow). × 2,600. (*c*) Higher magnification electron micrograph of the area in the box on *b*, but from a different section. The kinetochore of the manipulated chromosome is indicated by an arrow in the same orientation relative to the chromosome as in *b*. × 29,800.

nonkinetochore microtubules, but a few (4–5) are present in the KMt bundle of each of the other six manipulated chromosomes studied. As in cell 2, these nonkinetochore microtubules are almost invariably oblique rather than parallel to the kinetochore microtubules.

(*c*) The shape of the manipulated chromosome's bundle of kinetochore microtubules varies predictably with the angle at which the chromosome is stretched. If the manipulation needle is inserted in the chromosome and then moved so that the kinetochore remains pointed toward the pole, then almost all the KMts run straight to the pole (cell 1 and three others). If, instead, the needle is moved obliquely to the kinetochore-to-pole axis, so that the kinetochore points toward the middle of the spindle, then many KMts followed a curved path toward the pole and the kinetochore microtuble bundle has a hammock shape (cell 2, cell 3 [described below], and two others).

(*d*) Kinetochore microtubules of the chromosome nearest the manipulated chromosome are bent in the direction of the manipulated chromosome's kinetochore microtubules in six of the seven cells studied. The one exception is cell 2 in which by chance no chromosome was very close to the manipulated one (Fig. 4*b*). The number of kinetochore microtubules affected varies with the severity of the stress on the manipulated chromosome, from cell 1 in which most of the adjacent chromosome's KMts are bent to cells in which only 4 or 5 were bent. A "proximity rule" that the KMts closest to the manipulated chromosome are the most likely to be affected was examined in three cells. The results are given in Table I, along with the total number of KMts counted at the kinetochore. The last column in Table I ("out of place") gives the number of microtubules which are exceptions to the proximity rule: KMts which run straight toward the pole amidst curved ones (near the manipulated chromosome) or curved KMts amidst straight ones (farther from the manipulated chromosome). The total

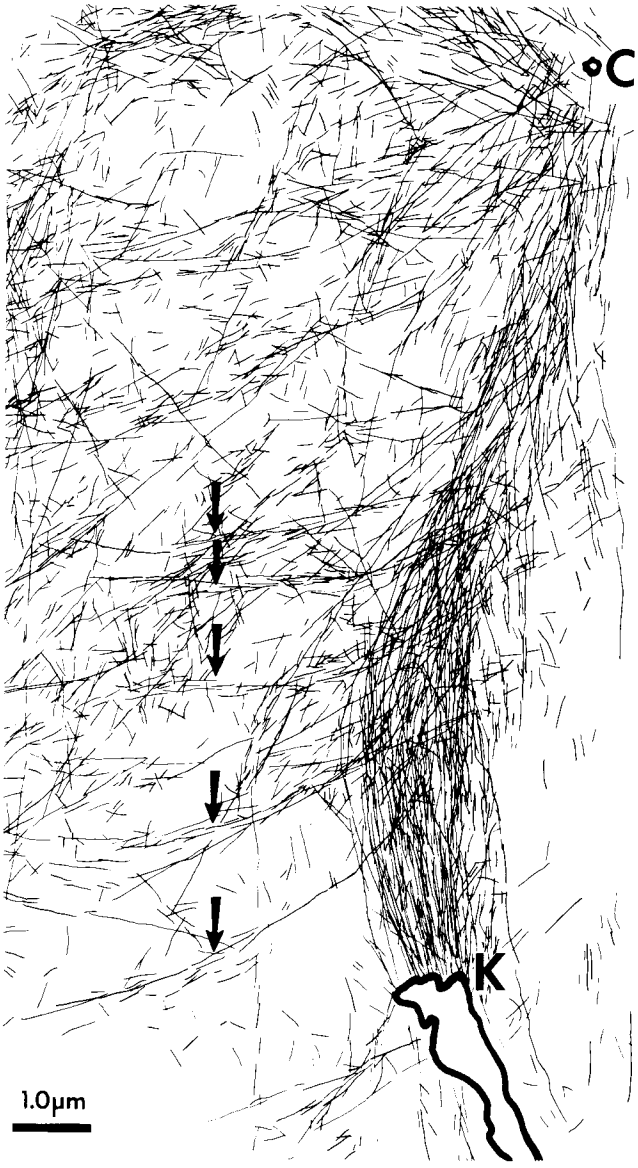

FIGURE 3 Two-dimensional reconstruction of the kinetochore end of the manipulated chromosome and associated microtubules in cell 2. The orientation is the same as in Fig. 4 *c*. The hammock-shaped kinetochore microtubule bundle extends between the kinetochore (*K*) and the centriole (*C*). Several nonkinetochore microtubules (arrows) run roughly perpendicular to the KMt bundle. The microtubules were traced from micrographs of 10 serial sections; both the kinetochore and the centriole occurred in the middle of this series of sections.

number of "out of place" microtubules is 9 out of 134 KMts for the three chromosomes in question. Thus, 7% of the total fail to obey the proximity rule—a small but not insignificant percent. Note also in Table I that when manipulated chromosomes are compared with adjacent chromosomes or chromosomes in a control cell (see first footnote, Table I), the total number of kinetochore microtubules varies, but in no consistent manner.

Chromosome Movement during Manipulation

Chromosome velocity during the micromanipulation experiment was determined in four of the five cells which supplied the most critical structural information (Table II; cell 2 was not included because the chromosome was stretched so short a time that a meaningful velocity determination was not possible). The velocity of the manipulated chromosome varied from normal to nil (Table II), depending on how much the chromosome was stretched. Unfortunately, structural clarity increases as functional capability decreases: the interrelations of microtubules are clearest in cell 1 in which the manipulated chromosome was brought to a halt. The manipulated chromosome did continue to move, though more slowly than usual (Table II), in two cells (4 and 5) which show all the structural features described for cell 1. Anaphase chromosome velocity in unmanipulated control cells is 0.5–0.7 μm/min (27). In cells 1 and 5 the velocity was significantly below this even for chromosomes some distance from the manipulated one. The decreased velocity in cell 1 probably was due to the manipulation, but for cell 5, the decrease was due to chromosome stickiness which retards chromosome separation in some cultured spermatocytes.

Kinetochore Microtubule Continuity and Associations between Kinetochore Microtubules

Most KMts of stretched chromosomes do not extend all the way from the kinetochore to the pole. This is suggested by simple inspection of the KMt bundle of the stretched chromosome in Fig. 2: the number of KMts appears to be much lower half way to the pole than at the kinetochore. A poleward decrease in KMt number has been verified in cells 1 and 5, in which the KMt bundle of the manipulated chromosome was well separated from other microtubules over much of its length and the number of microtubules was counted at various distances from the kinetochore (Table III). Even as little as 4 μm from the kinetochore, the number of microtubules is <80% of the number at 1 μm, whether the chromosome was moving (cell 5) or not (cell 1) when the cell was fixed. At 8 μm from the kinetochore in cell 1 (2.7 μm away from the pole, as calculated from the kinetochore-to-pole distance in Table IV), the number of microtubules is <40% of the number at 1 μm (Table III), or 43% of the number of KMts counted at the kinetochore (Table I). Thus, fewer than half the kinetochore microtubules can possibly span the whole kinetochore to pole distance, assuming the length present in life has been preserved.

These quantitative observations have been extended by tracking ten KMts and certain nearby microtubules throughout their length. Only those KMts having distinctive contours and/or positions were tracked—the sample is small, but every microtubule included could be tracked from one end to the other without ambiguity. Characterization of a few KMts was the sole aim, and hence frequency comparisons between KMts of different sorts are not reliable. In particular, most of the tracked KMts are shorter than the kinetochore-to-pole distance, but the sample may well be biased in favor of easily tracked, short KMts.

Most of the tracked microtubules are in cell 3, an extreme example of the consequences of applying tension oblique to the kinetochore-to-pole axis. The cell is shown before micromanipulation began in the 0.0-min print, Fig. 7. The microneedle was inserted into the chromosome and moved upward and to the left, causing the kinetochore to face the spindle equator rather than the pole (6.5-min print, Fig. 7). The tension was relaxed just before fixation, allowing the kinetochore to swing poleward (6.6- and 6.7-min prints, Fig. 7). Some microtubules associated with the manipulated chromosome are shown in Fig. 8. On the side of the KMt bundle nearer the spindle (right side, Fig. 8), remarkably curved microtubules

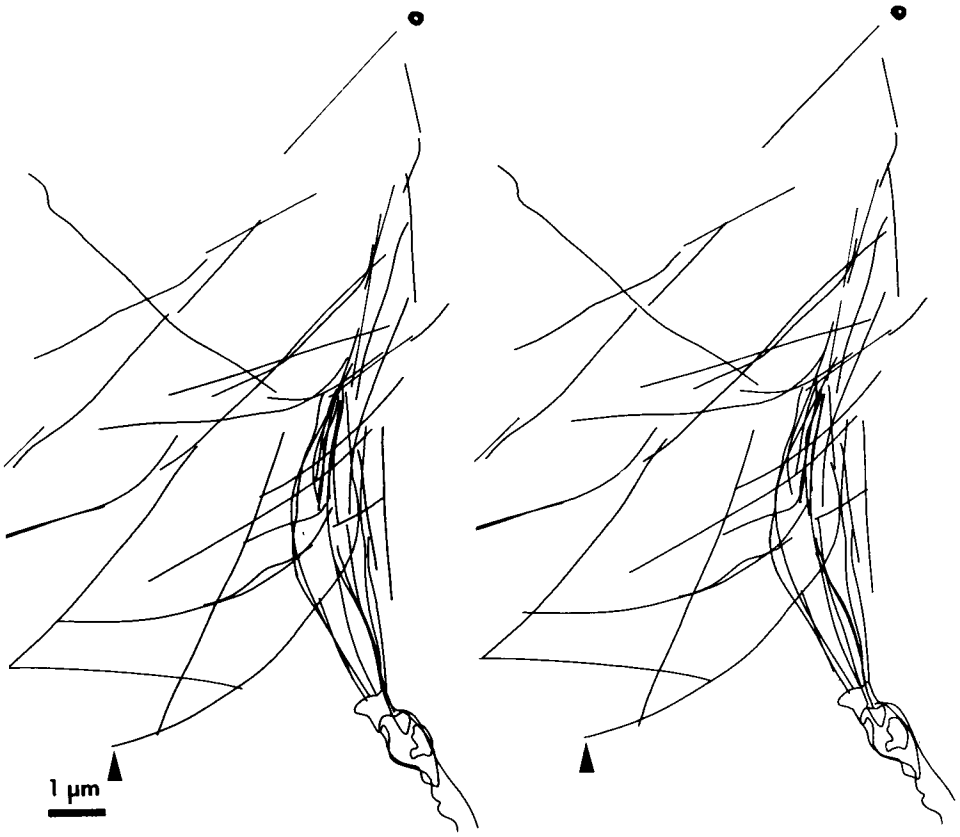

FIGURE 6 Three-dimensional reconstruction (stereo pair) of cell 2, showing the kinetochoric end of the manipulated chromosome, some of the associated microtubules, and one centriole. The orientation is the same as in Figs. 4 c and 5, and the same set of serial sections was used as for Fig. 5. Non-kinetochore microtubules enter the kinetochore microtubule bundle. Most pass on through, but one (arrowhead) curves to follow the path of the KMts. Every microtubule that enters the bundle has been traced to its true termination on the right (cytoplasmic) side, but only three have been traced as far as they actually extend toward the spindle on the right; all three ended withing the region shown in this figure.

TABLE I

*Number of Kinetochore Microtubules**

Cell number	Manipulated chromosome total	Adjacent chromosome			
		Total	Straight toward pole	Curved toward manipulated chro nosome	"Out of place"‡
1	49	41	8	33	5
4	39	41	18	23	2
5	38	52	38	14	2

* Counted at the kinetochore. The numbers of kinetochore microtubules for two chromosomes in an unmicromanipulated control cell were 55 and 42.
‡ See text for explanation.

TABLE II

Chromosome Velocity during Micromanipulation

Cell number	Velocity in μm/min		
	Micromanipulated chromosome	Adjacent chromosome	Next closest chromosome
1	0.0	0.2	0.2
3	0.2	0.4	0.4
4	0.2	0.3	0.6
5	0.2	0.2	0.2

run from the kinetochore toward the spindle before curving back toward the pericentriolar material. On the side toward the cell membrane, a KMt (labeled *1*, Fig. 8) extends poleward with relatively little curvature; for clarity, several other KMts with a similar path are not shown.

TABLE III

Kinetochore Microtubule Bundle of Two Manipulated Chromosomes

Cell number	Number of microtubules and percent of number at 1 μm		
	1 μm from kinetochore	4 μm from kinetochore	8 μm from kinetochore
1	55	35 (64%)	21 (38%)
5	53	41 (77%)	—

The KMts and certain nearby microtubules traced in their entirety fall into three classes:

(*a*) KMts which span the whole kinetochore to pole distance. One such KMt was tracked—microtubule 1 at the left in Fig. 8. The only other KMt of comparable length is microtubule 2 at the right in Fig. 8. Though microtubule 2 does not terminate at the pole, its length is only 0.6 μm less than the kinetochore-to-pole distance (Table IV).

(*b*) Shorter KMts, each closely associated with one other microtubule. The four KMts in this class are number 1 in Fig. 3 and numbers 3, 4, and 5 in Fig. 8. The associated microtubules are designated 1′, 3′, 4′ and 5′. As an example, consider pair 1/1′ in Fig. 3. KMt 1 can be traced in stereo view along a curved path from the kinetochore to its termination about two-thirds of the distance to the pole. Over the last 2–3 μm of its length, KMt 1 lies near microtubule 1′, which continues diagonally across the spindle to its termination amidst the KMts of the adjacent chromosome. The path of microtubule 1′ is a smooth, poleward continuation of the trajectory established by microtubule 1. Thus, the associated microtubule has been displaced and bent along with the KMt, which unmistakably reveals a

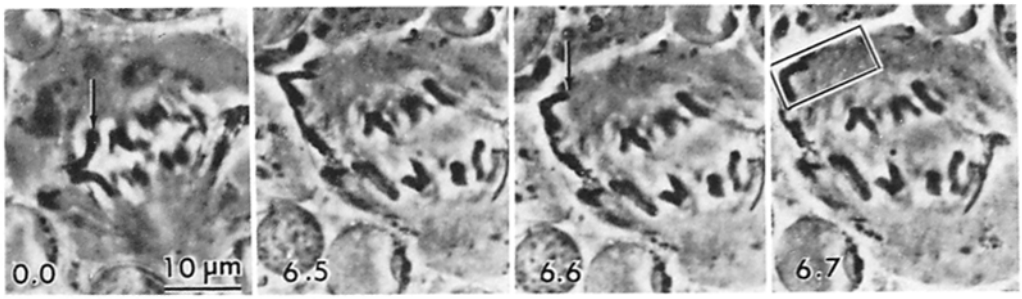

FIGURE 7 Prints from the ciné record of cell 3, showing the cell in life and after fixation. The time in minutes is given on each print, and the kinetochoric end of the manipulated chromosome is indicated by an arrow on the 0.0- and 6.6-min prints. The cell is shown in early anaphase before manipulation began (0.0-min print). At 2.0 min, the chromosome was moved up and to the left and moderately stretched as shown in the 6.5-min print, then released (6.6-min print), and the cell was fixed (6.7-min print). The chromosome was kept under tension for 4.6 min. The box on the 6.7-min print identifies the area shown in Fig. 8. × 1,000.

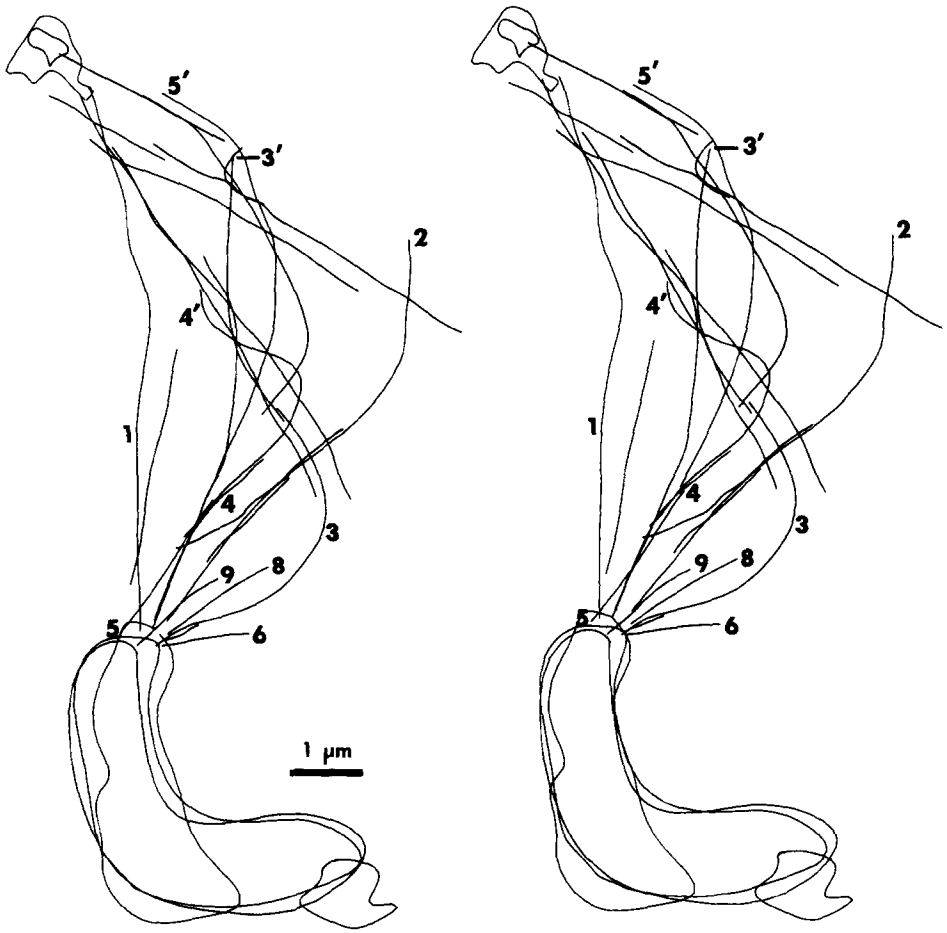

FIGURE 8 Three-dimensional reconstruction of cell 3. The region enclosed in the box in Fig. 7, 6.7-min print is shown, but rotated, so that the manipulated chromosome is at the bottom and pericentriolar material at the top. A few of the microtubules in this region are shown; some are remarkably bent. The microtubules identified by numbers have been traced in their entirety and fall into classes described in the text. Information from 11 sections was included in this reconstruction.

mechanical association between them. The spacing of microtubules 1 and 1′ in their zone of association is not entirely clear in Fig. 3. However, it is obvious in the micrographs of the individual sections that these microtubules are associated as follows: microtubule 1 and microtubule 1′ are close together laterally so that they appear to overlap in Fig. 3, but they are quite separate vertically—the apparently overlapped ends lie in adjacent serial sections, not the same section. The same is true of pairs 3/3′ and 5/5′, but in pair 4/4′, within part of the zone of overlap, the two microtubules lie in the same section. The overall length of each pair (Table IV) approximates the kinetochore-to-pole distance—the shortest pair is 1.2 μm shorter and the longest is 1.1 μm longer. Thus, each pair of these microtubules may originally have extended from the kinetochore to the pericentriolar material as a mechanically linked unit. If so, the pericentriolar end of microtubule 1′, for instance, was pulled out of the pericentriolar material by the tension on the chromosome during micromanipulation, and then was free to move to the position seen in Fig. 3.

(*c*) Short KMts not associated with other microtubules. Four very short KMts are seen at the right side of the kinetochore in Fig. 8. Three of these have been labeled 6, 8, and 9; number 7 (unlabeled) is the shortest, and lies between 6 and 8. Even the longest of these microtubules, number 8, is only one-fourth as long as the kinetochore-to-pole distance (Table IV). All four terminate in regions devoid of any other microtubules.

Beyond distinguishing types of KMts, a feature to note in Fig. 8 is the position of those microtubules with a free end

TABLE IV

Distance and Length Measurements

Cell number	Kinetochore to pole distance*	Microtubules‡	
		Number	Length
			μm
1 (Fig. 3)	10.7	1/1′	9.5
3 (Fig. 8)	7.6	1, 2	7.6, 7.0
		3/3′, 4/4′, 5/5′	8.6, 6.5, 8.7
		6, 7, 8, 9	1.3, 0.5, 1.8, 1.5

* Straight line distance between the kinetochore and the nearest mass of pericentriolar material.

‡ Where two microtubules are in question, 1 and 1′ for instance, the contour length from the kinetochoric end of microtubule 1 to the farther end of microtubule 1′ was measured, i.e., the length of the region in which 1 and 1′ overlap was counted only once, not twice. To conserve space, microtubules in the same class are listed on one line, followed by their lengths, listed in the same order.

distal to the kinetochore—an end not embedded in pericentriolar material. In unmanipulated spermatocytes, KMts run more or less straight toward the pole and are roughly parallel with one another. In Fig. 8, however, some microtubules (e.g., numbers 2, 3, and 6) have splayed out or been bent, and do not run directly toward the pole nor are they parallel to other microtubules. Thus, these microtubules are no longer part of a coherent bundle of kinetochore microtubules. The absence of evidence for strong interactions is particularly clear from the bent region of microtubule 3. If close linkages to other microtubules survived the stress on the chromosome, then either that region would not have bent or would have dragged other microtubules along with it. On the other hand, two groups of microtubules form sufficiently coherent bundles to suggest the possibility of weak lateral interactions among them: the groups of microtubules near the terminations of microtubules 4′ and 5′ are roughly parallel and lie at a distinctive angle. Note also that microtubules 4′ and 5′, though presumably displaced from their original positions, remain more closely associated with other microtubules than microtubules 2 and 6, for example.

Finally, the minimal radius of curvature a microtubule can sustain and yet remain intact is of some interest. The most sharply bent microtubule observed has a minimal radius of curvature of 0.25 μm (the bent region is just to the left of the poleward end of microtubule 3′, Fig. 8). The two bends in microtubule 4′ have radii of 0.5 and 0.75 μm, and five values for the next most sharply bent microtubules in Figs. 3 and 8 range from 1.25 to 2.0 μm.

DISCUSSION

Preservation of Spindle Microtubules

Our odd fixative—agar-treated glutaraldehyde—greatly improves microtubule preservation in grasshopper spermatocytes, and others who study large cells may wish to try it. (Improved fixation of smaller cells, including cultured mammalian cells, is unlikely—see Material and Methods.) Despite the improvement, we cannot assume that all the microtubules present in life have been preserved. Fortunately, many conclusions can be drawn solely from the microtubule configurations actually seen after chromosome micromanipulation, regardless of whether or not all microtubules were preserved. When conclusions are considered that do require an assumption about the preservation of microtubule number or length, the assumption will be made explicit and discussed. The only quantitative guide to microtubule preservation is to compare the number actually preserved with the number expected from measurements of spindle birefringence in living cells (see, e.g., references 25 and 34). Gratifyingly, the number of kinetochore microtubules in *Melanoplus* spermatocytes fixed in agar-treated glutaraldehyde averages 45 per chromosome (from Table I), and the number expected from birefrigence measurements is "about 45" (15).

Microtubules and Spindle Mechanical Properties

A spindle skeleton of some sort bears the load imposed when chromosomes move normally or when a chromosome is stretched with a micromanipulation needle (for review, see reference 24, pp. 241–242). Our results provide the first experimental electron microscope evidence that microtubules and whatever links them together are the spindle skeleton. Thus, the direction and magnitude of the stress on a chromosome manipulated in life is mirrored in the microtubule configurations observed after fixation. When a chromosome is shifted so that its kinetochore lies outside the spindle, its kinetochore microtubules are also shifted to this region. If the chromosome is then stretched with the microneedle, a stress is produced on its KMts and on the microtubules mechanically linked to them. If the chromosome is stretched along the kinetochore-to-pole axis, its KMts run straight toward the pole; if not, the KMt bundle is hammock-shaped. As the chromosome is increasingly stretched, the stress on its KMts increases, and more and more of the microtubules linked to its KMts are affected—bent—by the stress transmitted to them. With few exceptions, the microtubules closest to the manipulated chromosomes are affected most strongly, producing a gradient from more to less sharply bent microtubules across the spindle. These distorted microtubules are in fact due to stress on a chromosome some distance away and not to shifting of microtubules directly by the micromanipulation needle (see Material and Methods: the needle was never within the spindle).

These correlations of varied stress with altered microtubule configurations observed by electron microscopy are direct, but limited. The extensive light microscope studies of Begg and Ellis (1, 2) correlate birefringent spindle fibers with chromosome attachment to the spindle. Indirectly, but strongly, these studies also point to microtubules as the chief skeletal structures of the spindle (2).

Attachment of Chromosomes to the Spindle

Kinetochore microtubules in anaphase are firmly linked to other spindle microtubules only in the immediate vicinity of the pole. Stretching a chromosome before fixation makes this visible directly: KMts encounter large numbers of other spindle microtubules only near the pole (Figs. 2 and 3, and associated text). Chromosome attachment near the pole, mediated by flexible fibers, is just what was expected from earlier light microscope studies of micromanipulated chromosomes (1, 2, 29). Thus, chromosomes could easily be displaced from one side of the spindle to the other or pushed toward a pole in anaphase; but moving the needle away from the pole resulted in stretching the chromosome without much increase in the kinetochore-to-pole distance. Significantly, these manipulations could be done without interfering with normal chromosome movement (1, 2, 29) and thus suggest that connections near the pole suffice for normal chromosome attachment and movement. In our work, we found that stress on a chromosome sufficient to slow or stop its movement was necessary for clarity

in the electron microscope analysis. Hence the wording of the conclusion: "firm" connections (i.e., those surviving the stress imposed) are limited to the polar regions. Any weaker linkages, disrupted by the stress in the present experiments, probably are not essential for normal spindle function. Parenthetically, note that micromanipulation/electron microscope observations on the region of KMt linkage to the spindle are limited to anaphase and may not apply to other stages, particularly prometaphase.

Some non-KMts do enter the KMt bundle nearer to the kinetochore than the region of general commingling near the pole (Figs. 5 and 6). Most of these non-KMts are not intimately associated in space with KMts and appear to have been dragged along as the KMt bundle was displaced, without much resisting the displacement. They may simply be entangled with kinetochore microtubules or embedded in a common gel, as discussed below. In any case, this class of non-KMts plainly lacks specific, close linkages to KMts, and whatever their significance, they make at most only a minor contribution to the attachment of chromosomes to the spindle.

Some earlier electron microscope studies showed that KMts commingle with other spindle microtubules mainly near the pole. However, even in the clearest examples from whole cells (e.g., references 5, 30), some non-KMts were found near KMts in the region closer to the kinetochore. In these cases, the absence of experimentally applied stress before fixation makes it is impossible to distinguish between mere contiguity in space and genuine mechanical linkage. Partially disrupted isolated spindles provide clearer evidence that KMts are firmly anchored only near the pole (20), but the loss of other linkages during spindle isolation and subsequent treatment cannot be excluded.

Kinetochore Microtubules

CONTINUITY: Fewer than half the KMts extend all the way to the pole at anaphase in micromanipulated grasshopper spermatocytes, and some are very short. Some short KMts may have resulted from breakage due to stress during micromanipulation or from failure to preserve the full length present in life. Breakage might result from micromanipulation if microtubules are bent to the point of fracture, in which case one would expect to see long, sharply bent microtubules as well as short, fractured segments. This seems an unlikely source of short microtubules except, perhaps, in cells with numerous bent microtubules (e.g., Fig. 8). Neither breakage nor failure of preservation is a likely source of the short KMts associated with a second microtubule. These pairs of microtubules share a common distinctive trajectory in the region of their association which unmistakably shows a mechanical linkage between them, and together each pair spans a distance approximately equal to the kinetochore-to-pole distance. Hence originally the distal end of each pair may well have terminated in pericentriolar material, although as seen after micromanipulation, they terminate a variable distance away. These microtubule pairs thus appear to represent natural units which probably link kinetochore and pole in unmanipulated cells, and hence the KMt member of each pair is credible as a truly short KMt. If the original length of these short KMts has been preserved, then very likely so has that of other KMts. Also relevant is the concordance between KMt number and birefringence. We tentatively conclude that numerous short KMts do exist in anaphase spindles of grasshopper spermatocytes. The class of KMts associated pairwise with a second microtubule deserves additional study because of its potential importance in linking the kinetochore with the pole in cells with short KMts.

FIGURE 9 "Hinge-anaphase": the separation of chromosomes nearest the pair stuck-together (at the left) was less than those farther away. From Bělař (3), 1929, with the publisher's permission. (Reproduced upside-down from the original orientation to facilitate comparison with Fig. 2).

Other cell types also may have numerous KMts which do not span the whole kinetochore-to-pole distance (for review, see reference 7, and for recent observations, 14 and 35). Counterexamples exist, however. In some fungi, most KMts probably extend from kinetochore to pole (e.g., reference 33), and in mammalian cell lines, ~50% certainly do in cold-treated cells (31), and >90% during recovery from colcemid treatment (38). For KMts unambiguously tracked from kinetochore to pole, as in these instances, there can be no doubt that the true length of microtubules has been preserved. Hence, while it appears that either short or long KMts may predominate in various cells, additional studies are badly needed.

KINETOCHORE MICROTUBLE BUNDLE: The coherence of KMts and associated microtubules to form a more or less discrete bundle depends on the anchorage of microtubule ends and on lateral interactions along their length. In anaphase, KMts are firmly anchored at the kinetochore and probably less firmly at the pole (this report; see also references 27 and 29; in prometaphase, the anchorage of KMts at the kinetochore is fragile [25, 27]).

Lateral interactions among the microtubules of the KMt bundle are revealed by configurations such as those in Fig. 8. Generally, lateral interactions are weak, but real—many microtubules splay out if one end is unanchored, but microtubules are also seen in groups suggesting some sort of mechanical association. We conclude that coherence of the KMt bundle at anaphase is primarily determined by anchorage of microtubule ends. The distribution of anchorage sites within the kinetochore and at or near the pole determines the spacing of microtubules at the ends of the bundle, and this, plus weak lateral interactions in between, gives the KMt bundle the degree of structural and mechanical coherence it possesses.

Mechanical Associations across the Spindle

Perhaps the most intriguing effect of stretching one chromosome is the distortion of the kinetochore microtubules of the adjacent chromosome. The mechanical association this reveals provides an explanation for a particularly interesting example of interdependent chromosome movement—the so-called "hinge anaphase" described by Bělař (3) and Ris (32) and others. An example is shown in Fig. 9. If a chromosome pair at one side of the spindle (the left pair in Fig. 9) is stuck together and fails to separate, the separation of adjacent pairs is also reduced, even though they themselves are not stuck together. Farther away, chromosome separation is more nearly normal, and thus separation increases in a gradient from the stuck-together pair. Now compare the gradient in separation (Fig. 9) with the gradient in distortion of microtubules after a chromosome is stretched with a microneedle (Fig. 2). The mechanical situation is similar: in both cases the stress on the spindle is greater than normal, though the stress is produced

internally in one case (by the spindle itself, as it stretches stuck-together chromosomes) and externally in the other (by a microneedle stretching a chromosome). We suggest that in both situations spindle organization is disrupted by the stress, and the disruption spreads in a gradient from where the stress was applied because adjacent spindle regions are mechanically associated: the stress is locally applied but has nonlocal consequences on spindle integrity. The stress might affect either force production itself or the spindle skeleton, which would reduce the spindle's capacity to translate force production into directed chromosome movement. In either case, the mechanical association across the spindle we have observed helps in understanding how a reduced rate or extent of chromosome movement in one chromosome pair affects nearby chromosomes otherwise free to move normally.

The Nature of Mechanical Associations among Microtubules

The mechanical associations of microtubules made visible by stretching a chromosome do not display the characteristics expected for linkage by dynein or any similar, specific microtubule cross-bridging molecule. Dynein links doublet microtubules in cilia and flagella, and singlet microtubules in vitro, microtubule-by-microtubule, to give a wall-to-wall separation of 15–20 nm uniformly along their lengths (e.g., 8, 37). Microtubules in one part of the spindle—the middle of the interzone—show such spacing, and cross-bridges between spindle microtubules have sometimes been seen (for review, see reference 17). The following discussion concerns microtubule associations only in the large but limited region of the spindle open to analysis after the present micromanipulation experiments—the regions near each pole and at the middle of the interzone are excluded.

The kinetochore microtubules of adjacent chromosomes provide a particularly clear example of unmistakable mechanical association in the apparent absence of cross-bridges between nearby microtubules. Stress on the KMts of one chromosome bends the KMts of the adjacent chromosome even though no microtubules close to the bent ones and having the same contour are seen (Figs. 2 and 3). The immediate question is whether short linkages did in fact connect these microtubules in life, but somehow were lost. Two possibilities are evident. First, short linkages might have been broken by the stress applied. If this were true, one might still expect to see closely appressed microtubules toward the pole—beyond the point where the linkages were broken, but still within the analyzable region before the thicket of microtubules at the pole. This has never been observed. More telling, the elegant study of Mizushima et al. (21) shows that the elastic resistance of microtubules to bending is relatively great, and hence microtubules shorter than ~150 μm behave like rigid rods in vitro. Hence, bent microtubules would be expected to return to their original straight conformation if the linkers responsible for the bending subsequently ruptured. At a minimum, some constraints on microtubule shape not present in vitro would be necessary to explain the retention of the bent configuration. Second, microtubules may have been lost during preparation for electron microscopy—microtubules that in life ran between the KMts of adjacent chromosomes with cross-bridges linking one set of KMts to the other. The absence of even a trace of the required microtubules, in spindles containing every type of microtubule now known, argues against this possibility. So does the quantitative agreement between birefringence and KMt number. We conclude that while short cross-bridges cannot be rigorously excluded, a plausible alternative would merit serious consideration.

If short, microtubule-by-microtubule linkages do not connect the microtubules in question, what does? Simple entanglement of microtubules with one another can be dismissed. Entangled microtubules should be directly visible as such, when viewed after stress in life, and none are seen (Figs. 2 and 3; even the ambiguous hints of entanglement recognized for non-KMts in the KMt bundle are absent). A spindle matrix with the properties of a gel (18) is the most attractive source of the associations observed. Embedment of microtubules in a gel would associate them more diffusely than microtubule-to-microtubule cross-bridges: microtubules would be associated group-by-group rather than microtubule-by-microtubule. Thus, stress on one group of microtubules would be transmitted by the gel to nearby microtubules and distort them as a group, though those closest to the source of stress would be the most affected. However, exceptions to this "proximity rule" should be expected, since the structural/mechanical relationships of microtubules in a gel would not likely be highly regular. The microtubule configurations observed match these expectations. Most significant, if a gel is responsible, then the configurations themselves show that the gel is sufficiently cohesive mechanically to be of interest for mitosis—it is capable of transmitting a force great enough to bend microtubules. McIntosh (18) has suggested that a gel-like "net," mechanically coupled to microtubules, may generate the forces that move chromosomes. Our results obviously have no direct bearing on the validity of this model, but they do suggest that the required mechanical coupling of microtubules by a gel may be present.

In conclusion, the application of stress before fixation reveals mechanical associations among spindle microtubules which in unaltered cells might at best be only surmised from the character of microtubule association in space. Our study leaves unresolved the nature of microtubule associations near the poles and in the middle of the interzone at anaphase—regions of crucial importance for chromosome attachment to the spindle and movement. The investigation of those regions by micromanipulation combined with electron microscopy will require greater disruption of normal spindle structure and function than was necessary here. Controlled disruption, however, is the virtue as well as the limitation of successful dissection whether in gross or microscopic anatomy.

The three-dimensional reconstructions in this report were made at York University, Toronto, in the laboratory of Peter Moens. We thank Peter and Ted Moens for exceptional generosity in sharing their computer facilities and programs. We also thank Kent McDonald for permission to cite unpublished results on microtubule preservation in PtK_2 cells, John Boynton for sharing his electron microscope facilities, and Montrose Moses for use of an electronic planimeter.

This investigation was supported in part by grants GM 13745 and GM 27569 from the Institute of General Medical Sciences, National Institutes of Health, and by grant PCM 79-11481 from the Division of Physiology, Cell and Molecular Biology, National Science Foundation.

Received for publication 1 April 1982, and in revised form 21 June 1982.

REFERENCES

1. Begg, D. A., and G. W. Ellis. 1979. Micromanipulation studies of chromosome movement. I. Chromosome-spindle attachment and the mechanical properties of chromosome spindle fibers. *J. Cell Biol.* 82:528–541.
2. Begg, D. A., and G. W. Ellis. 1979. Micromanipulation studies of chromosome movement. II. Birefringent chromosomal fibers and the mechanical attachment of chromosomes to the spindle. *J. Cell Biol.* 82:542–554.

3. Bělař, K. 1929. Beiträge zur Kausalanalyse der Mitose. II. Untersuchungen an den Spermatocyten von *Chorthippus* (*Stenobothrus*) *lineatus* Panz. *Wilhelm Roux' Arch. Entwicklungsmech. Org.* 118:359–484.
4. Cande, W. Z. 1982. Nucleotide requirements for anaphase chromosome movements in permeabilized mitotic cells: anaphase B but not anaphase A requires ATP. *Cell.* 28:15–22.
5. Dietrich, J. 1979. Reconstructions tridimensionnelles de l'appareil mitotique à partir de coupes sériées longitudinales de méiocytes polliniques. *Biol. Cell.* 34:77–82.
6. Forer, A., and B. R. Brinkley. 1977. Microtubule distribution in the anaphase spindle of primary spermatocytes of a crane fly (*Nephrotoma suturalis*). *Can. J. Genet. Cytol.* 19:503–519.
7. Fuge, H. 1977. Ultrastructure of the mitotic spindle. *Int. Rev. Cytol. Suppl.* 6:1–58.
8. Haimo, L. T., B. R. Telzer, and J. L. Rosenbaum. 1979. Dynein binds to and crossbridges cytoplasmic microtubules. *Proc. Natl. Acad. Sci. U. S. A.* 76:5759–5763.
9. Jensen, C. G. 1982. Dynamics of spindle microtubule organization: kinetochore fiber microtubules of plant endosperm. *J. Cell Biol.* 92:540–558.
10. Kubai, D. F. 1973. Unorthodox mitosis in *Trichonympha agilis*: kinetochore differentiation and chromosome movement. *J. Cell Sci.* 13:511–552.
11. Kubai, D. F., and D. Wise. 1981. Nonrandom chromosome segregation in *Neocurtilla* (*Gryllotalpa*) *hexadactyla*: an ultrastructural study. *J. Cell Biol.* 88:281–293.
12. LaFountain, J. R. 1974. Birefringence and fine structure of spindles in spermatocytes of *Nephrotoma suturalis* at metaphase of first meiotic division. *J. Ultrastruct. Res.* 46:268–278.
13. LaFountain, J. R. 1976. Analysis of birefringence and ultrastructure of spindles in primary spermatocytes of *Nephrotoma suturalis* during anaphase. *J. Ultrastruct. Res.* 54:333–346.
14. LaFountain, J. R., and L. A. Davidson. 1980. An analysis of spindle ultrastructure during anaphase of micronuclear division in *Tetrahymena*. *Cold Spring Harbor Conf. Cell Proliferation.* 3 (Book A):41–61.
15. Marek, L. F. 1978. Control of spindle form and function in grasshopper spermatocytes. *Chromosoma (Berl.).* 68:367–398.
16. McDonald, K. L., M. K. Edwards, and J. R. McIntosh. 1979. Cross-sectional structure of the central mitotic spindle of *Diatoma vulgare*: evidence for specific interactions between antiparallel microtubules. *J. Cell Biol.* 83:443–461.
17. McIntosh, J. R. 1979. Cell division. *In* Microtubules. K. Roberts and J. S. Hyams, editors. Academic Press, London. 381–441.
18. McIntosh, J. R. 1981. Microtubule polarity and interaction in mitotic spindle function. *In* International Cell Biology 1980–81. H. G. Schweiger, editor. Springer-Verlag, Berlin. 359–368.
19. McIntosh, J. R., K. L. McDonald, M. K. Edwards, and B. M. Ross. 1979. Three-dimensional structure of the central mitotic spindle of *Diatoma vulgare*. *J. Cell Biol.* 83:428–442.
20. McIntosh, J. R., J. E. Sisken, and L. K. Chu. 1979. Structural studies on mitotic spindles isolated from cultured human cells. *J. Ultrastruct. Res.* 66:40–52.
21. Mizushima, J., S. Yamazaki, T. Maeda, and T. Miki-Noumura. 1982. Flexibility of singlet microtubule. *In* Biological Functions of Microtubules and Related Structures. H. Sakai, H. Mohri, and G. G. Borisy, editors. Academic Press, Tokyo. In press.
22. Moens, P. B., and T. Moens. 1981. Computer measurements and graphics of three-dimensional cellular ultrastructure. *J. Ultrastruct. Res.* 75:131–141.
23. Moore, M. J. 1975. Removal of glass coverslips from cultures flat embedded in epoxy resins using hydrofluoric acid. *J. Microsc.* 104:205–207.
24. Nicklas, R. B. 1971. Mitosis. *In* Advances in Cell Biology. D. M. Prescott, L. Goldstein, and E. McConkey, editors. Appleton-Century-Crofts, New York. 2:225–297.
25. Nicklas, R. B., B. R. Brinkley, D. A. Pepper, D. F. Kubai, and G. K. Rickards. 1979. Electron microscopy of spermatocytes previously studied in life: Methods and some observations on micromanipulated chromosomes. *J. Cell Sci.* 35:87–104.
26. Nicklas, R. B., T. S. Hays, and D. F. Kubai. 1979. A new approach to the organization of the mitotic spindle. *J. Cell Biol.* 83(2, Pt. 2):375*a* (Abstr.).
27. Nicklas, R. B., and C. A. Koch. 1972. Chromosome micromanipulation. IV. Polarized motions within the spindle and models for mitosis. *Chromosoma (Berl.).* 39:1–26.
28. Nicklas, R. B., D. F. Kubai, and T. S. Hays. 1982. Spindle structure after chromosome micromanipulation. *In* Biological Functions of Microtubules and Related Structures. H. Sakai, H. Mohri, and G. G. Borisy, editors. Academic Press, Tokyo. In press.
29. Nicklas, R. B., and C. A. Staehly. 1967. Chromosome micromanipulation. I. The mechanics of chromosome attachment to the spindle. *Chromosoma (Berl.).* 21:1–16.
30. Peterson, J. B., and H. Ris. 1976. Electron-microscopic study of the spindle and chromosome movement in the yeast *Saccharomyces cerevisiae*. *J. Cell Sci.* 22:219–242.
31. Rieder, C. L. 1981. The structure of the cold-stable kinetochore fiber in metaphase PtK_1 cells. *Chromosoma (Berl.).* 84:145–158.
32. Ris, H. 1949. The anaphase movement of chromosomes in the spermatocytes of the grasshopper. *Biol. Bull. (Woods Hole).* 96:90–106.
33. Roos, U.-P. 1980. The spindle of cellular slime molds. *In* Microtubules and Microtubule Inhibitors 1980. M. De Brabander and J. De Mey, editors. Elsevier/North-Holland, Amsterdam. 385–398.
34. Sato, H., G. W. Ellis, and S. Inoué. 1975. Microtubular origin of mitotic spindle form birefringence. Demonstration of the applicability of Wiener's Equation. *J. Cell Biol.* 67:501–517.
35. Schibler, M. J., and J. D. Pickett-Heaps. 1981. Kinetochore bundle structure in the green alga, *Oedogonium*. *J. Cell Biol.* 91(2, Pt. 2):316*a* (Abstr.).
36. Schrader, F. 1953. Mitosis: The Movement of Chromosomes in Cell Division. Second Edition. Columbia University Press, New York.
37. Warner, F. D. 1978. Cation-induced attachment of ciliary dynein cross-bridges. *J. Cell Biol.* 77:R19–R26.
38. Witt, P. L., H. Ris, and G. G. Borisy. 1981. Structure of kinetochore fibers: microtubule continuity and inter-microtubule bridges. *Chromosoma (Berl.).* 83:523–540.